Available online at www.sciencedirect.com
ScienceDirect
Journal of Solid State Chemistry 181 (2008) 637–645
JOURNAL OF SOLID STATE CHEMISTRY
www.elsevier.com/locate/jssc

Hydrothermal synthesis and structural characterization of two 1-D and 2-D Dawson-based phosphotungstates

Jun-Wei Zhao[a], Shou-Tian Zheng[a], Wei Liu[b], Guo-Yu Yang[a,*]

[a]*State Key Laboratory of Structural Chemistry, Fujian Institute of Research on the Structure of Matter, Graduate School of the Chinese Academy of Sciences, Fuzhou, Fujian 350002, PR China*
[b]*College of Material Science and Engineering, Shandong University of Technology, Zibo, Shangdong 255049, PR China*

Received 13 September 2007; received in revised form 26 December 2007; accepted 2 January 2008
Available online 9 January 2008

Abstract

Two new Dawson-based phosphotungstates $(H_2en)_{0.5}H[Cu(en)_2(H_2O)]_2\{[Cu(en)_2](\alpha_1\text{-}P_2W_{17}CuO_{61})\}\cdot 8H_2O$ (**1**) (en = ethylenediamine) and $[4,4'\text{-}H_2bpy]_2\{[Cu(4,4'\text{-}bpy)_3][Cu(4,4'\text{-}bpy)_4(H_2O)_2]_2[Cu(4,4'\text{-}bpy)][\alpha\text{-}P_2W_{18}O_{62}]_2\}\cdot 6H_2O$ (**2**) (4,4′-bpy = 4,4′-bipyridine) have been hydrothermally synthesized and structurally characterized. **1** crystallizes in the triclinic space group $P\bar{1}$ with $a = 11.7626(17)$, $b = 13.246(2)$, $c = 29.350(5)$ Å, $\alpha = 87.355(5)$, $\beta = 79.583(5)$, $\gamma = 66.993(3)^\circ$, $V = 4138.3(11)$ Å^3, $Z = 2$, GOF = 1.089, $R_1 = 0.0563$ and $wR_2 = 0.1505$, whereas **2** belongs to the orthorhombic space group *Iba*2 with $a = 22.277(8)$, $b = 47.04(2)$, $c = 22.153(8)$ Å, $V = 23215(17)$ Å^3, $Z = 4$, GOF = 1.051, $R_1 = 0.0627$ and $wR_2 = 0.1477$. **1** consists of a 1-D linear chain structure constructed from monocopper^{II}-substituted Dawson polyoxoanions, while **2** represents the first 2-D sheet-like structure with a (4,4)-connected topological net built up from plenary Dawson-type polyoxoanions and Cu^{II}-4,4′-bpy complex cations in polyoxometalate chemistry.

Keywords: Polyoxometalates; Dawson structure; Hydrothermal reaction; Copper

1. Introduction

The widespread contemporary interest in the design and syntheses of inorganic–organic hybrid materials reflects their intriguing structural features and surprising compositional variability as well as their extensive theoretical and practical application in such fields as catalysis, absorption, electric, optical and magnetic materials [1–7]. Recently, polyoxometalates (POMs), as one kind of significant metal oxide clusters, have been widely employed as important molecular building blocks to construct inorganic–organic hybrid materials [8–13]. Hitherto, the most employed POM candidates are the saturated Keggin-type polyoxoanions, which can be formulated as $[XM_{12}O_{40}]^{n-}$ (X = P^V, As^V, Si^{IV}, Ge^{IV} or B^{III}; M = Mo^{VI}, W^{VI} or Nb^V), partly because the charge density of the surface oxygen atoms on them can be increased either by reducing some metal centers or replacing higher-valent metal centers with lower-valent metal centers [14]. Such typical examples include $[Ni(phen)_3][PMo_9^{VI}Mo_3^VO_{40}\{Ni(phen)\}_2]$ [15], $[Ni(2,2'\text{-}bpy)_3]_{1.5}[PW_{10}^{VI}W_2^VO_{40}Ni(2,2'\text{-}bpy)_2(H_2O)]$ [16] and $[4,4'\text{-}H_2bpy][Cu(4,4'\text{-}bpy)]_2[HPCuMo_{11}O_{39}]$ [17]. To date, the saturated Keggin-type POM candidates have been extensively investigated to lead to a family of inorganic–organic hybrid materials containing 0-, 1-, 2- and even 3-D structures assembled from saturated Keggin polyoxoanions and metal-organic cations [18–25]. For example, $[Ni(4,4'\text{-}Hbpy)_2(4,4'\text{-}bpy)(H_2O)_2](SiW_{12}O_{40})\cdot 6H_2O$ (0-D) [21], $\{[Cu(4,4'\text{-}bpy)]_3[HSiMo_{12}O_{40}]\}\cdot 1.5H_2O$ (1-D) [23], $\{[Cu(4,4'\text{-}bpy)]_4[SiW_{12}O_{40}]\}\cdot 3H_2O$ (2-D) [23] and $[Ag(4,4'\text{-}bpy)](OH)\{[Ag(4,4'\text{-}bpy)]_2[PAgW_{12}O_{40}]\}\cdot 3.5H_2O$ (3-D) [24]. In contrast, the investigation on inorganic–organic hybrid materials based on saturated Dawson-type polyoxoanions ($[X_2M_{18}O_{62}]^{n-}$ (X = P^V or As^V; M = Mo^{VI} or W^{VI}) remain much less developed [6,26–30]: only several examples such as $[\{Ce(DMF)_4(H_2O)_3\}\{Ce(DMF)_4(H_2O)_4\}(P_2W_{18}O_{62})]\cdot H_2O$ (1-D) [6], $[\{La(DMF)_6(H_2O)\}\{La(DMF)_{4.5}(H_2O)_{2.5}\}(P_2W_{18}O_{62})]$ (1-D) [6], $[Gd(DMF)_6(H_2O)_2]_2[P_2W_{18}O_{62}]\cdot 4DMF\cdot 2H_2O$ (0-D) [26], $[Ce(NMP)_3(H_2O)_5][Ce(NMP)_3$

*Corresponding author. Fax: +86 591 8371 0051.
E-mail address: ygy@fjirsm.ac.cn (G.-Y. Yang).

0022-4596/$ - see front matter © 2008 Elsevier Inc. All rights reserved.
doi:10.1016/j.jssc.2008.01.002

$(H_2O)_4][(P_2W_{18}O_{62})]\cdot 4H_2O$ (0-D) [26], [{Gd(DMF)$_6$}{Gd(DMF)$_7$}$(P_2W_{18}O_{62})]\cdot 0.5$DMF (1-D) [26], $H_{1.5}$[Sm$(H_2O)_8]_{0.5}$[Sm$(DMF)_6(H_2O)$ $(P_2W_{18}O_{62})]\cdot DMF\cdot 3H_2O$ (1-D) [27], [{Cu_2(2,4′-Hbpy)$_4$}$As_2Mo_{18}O_{62}]\cdot 2H_2O$ (1-D) [28], [Cu^{II}(en)(2,2′-bpy)]$_3$ $[P_2W_{18}O_{62}]\cdot 3H_2O$ (0-D) [29], [Zn(phen)$_2(H_2O)_2$][{Zn(phen)$_2$}{Zn(phen)$_2(H_2O)$}{$P_2W_{18}O_{62}$}]$\cdot 8H_2O$ (1-D) [30] and [Cd(phen)$_2(H_2O)_2$][{Cd(phen)$_2$}{Cd(phen)$(H_2O)_3$}{$P_2W_{18}O_{62}$}]$\cdot 4H_2O$ (1-D) [30]. Thus it can be seen that these saturated Dawson-type compounds are 0- or 1-D structures. In addition, several monovacant Dawson-type compounds have been reported in 2001 and 2006 [31,32], such as [Cu(en)$_2(OH_2)]_2$[H_2en][{Cu(en)$_2$}$P_2CuW_{17}O_{61}]\cdot 5H_2O$ (1-D) [31], [Cu(en)$_2(OH_2)]_2$[Cu(en)$_2]_{0.5}$[H_2en]$_{0.5}$[{Cu(en)$_2$}$P_2CuW_{17}O_{61}]\cdot 5H_2O$ (1-D) [31], KNa_3[Nd_2 $(H_2O)_{10}(P_2W_{17}O_{61})]\cdot 11H_2O$ (0-D) [32], (H_3O)[$Nd_3(H_2O)_{17}(P_2W_{17}O_{61})]\cdot 6.75H_2O$ (0-D) [32], (4,4′H_2bpy)$_2$[Ln_2 $(H_2O)_9(P_2W_{17}O_{61})]\cdot nH_2O$ (Ln = Nd, La, Eu) (2-D) [32]. To the best of our knowledge, only one 2-D inorganic–organic hybrid structure based on saturated Dawson-type polyoxoanions $(NH_4)_3$(4,4′-H_2bpy)[Cu^{I}(4,4′-bpy)]$_7$ $[P_2W_{18}O_{62}]_2\cdot 10H_2O$ has been recently reported by Jin et al. [29]. Therefore, the exploration and construction of high-dimensional Dawson-type compounds remain a long-standing challenge for synthetic chemists, and further research is necessary to enrich and develop this branch. Currently, we are exploiting the reaction of lacunary POM precursors with transition-metal (TM) cations under hydrothermal conditions and have obtained a class of novel inorganic–organic hybrid polyoxotungstate (POTs) $[[Ni(L)_2]_m[\{Ni_6(\mu_3\text{-}OH)_3(L)_{3-n}(H_2O)_{6+2n}\}(B\text{-}\alpha\text{-}XW_9O_{34})]\cdot yH_2O$ (L = organodiamines, $X = P^{V}$, Si^{IV}) and [{$Ni_7(\mu_3$-OH)$_3O_2$(dap)$_3(H_2O)_6$}(B-α-PW_9O_{34})][{$Ni_6(\mu_3$-OH)$_3$(dap)$_3(H_2O)_6$}(B-α-PW_9O_{34})][Ni(dap)$_2(H_2O)_2]\cdot 4.5H_2O$ based on a single trivacant Keggin fragment capped by a hexa-Ni^{II} or hepta-Ni^{II} unit [33,34]. Moreover, we have also obtained a family of inorganic–organic hybrid tetra-TM^{II} sandwiched POTs with discrete or 2-D structures [35–37]. Meanwhile, two novel hexa-Cu^{II} substituted POTs [$Cu_6(\mu_3$-OH$)_3$(en)$_3$ $(H_2O)_3$(B-α-PW_9O_{34})]$\cdot 7H_2O$ [34] and [Cu(dap)$_2]_2$[{[Cu(dap)$_2$ $(H_2O)]_2$[Cu_6(dap)$_2$(B-α-$SiW_9O_{34})_2$]}$\cdot 4H_2O$ [38] were also isolated. Furthermore, three unprecedented octa-Cu^{II} sandwiched POTs [Cu(dap)$(H_2O)_3]_2$[{Cu_8(dap)$_4(H_2O)_2$}(B-α-$SiW_9O_{34})_2$]$\cdot 6H_2O$ [34] and [Cu$(H_2O)_2]H_2$[Cu_8(dap)$_4(H_2O)_2$ (B-α-$XW_9O_{34})_2$] ($X = Si^{IV}$, Ge^{IV}) [39] have been separated in our lab. As a part of our recent work, in the present paper, we report two Dawson-based phosphotungstates $(H_2en)_{0.5}$H[Cu(en)$_2(H_2O)]_2$[{Cu(en)$_2$}(α$_1$-$P_2W_{17}CuO_{61}$)]$\cdot 8H_2O$ (**1**) and [4,4′-H_2bpy]$_2$[{Cu(4,4′-bpy)$_3$][Cu(4,4′-bpy)$_4(H_2O)_2]_2$ [Cu(4,4′-bpy)][α-$P_2W_{18}O_{62}]_2$}$\cdot 6H_2O$ (**2**). **1** contains a 1-D linear chain constructed from monocopper^{II}-substituted Dawson polyoxoanions, where the 1-D chain architecture is almost the same to those in [Cu(en)$_2(OH_2)]_2$[H_2en][{Cu(en)$_2$}$P_2CuW_{17}O_{61}]\cdot 5H_2O$ (**3**) [31] and [Cu(en)$_2(OH_2)]_2$[Cu(en)$_2]_{0.5}$ [H_2en]$_{0.5}$[{Cu(en)$_2$}$P_2CuW_{17}O_{61}]\cdot 5H_2O$ (**4**) [31], while **2** represents the first 2-D sheet-like structure with a (4,4)-connected topological net built up from plenary Dawson-type polyoxoanions and Cu^{II}-4,4′-bpy complex cations in the POM chemistry. In **2**, there are three crystallographically unique copper ions (Cu1, Cu2 and Cu3). Interestingly, the [α-$P_2W_{18}O_{62}]^{6-}$, Cu1 and Cu3 ions arrange in the helical distribution motif along the [100] direction generating the helical chain structures. Adjacent two helical chains have the opposite handedness.

2. Experimental

2.1. Materials and physical measurements

The lacunary POM precursors K_{12}[α-$H_2P_2W_{12}O_{48}]\cdot 24H_2O$ and Na_{12}[α-$P_2W_{15}O_{56}]\cdot 24H_2O$ were prepared according to the literature [40] and their purities were identified by IR spectra. All other chemicals were obtained from commercial sources and used without further purification. Infrared spectra of solid samples were obtained as KBr pellets on an ABB Bomen MB 102 FT-IR spectrometer in the 4000–400 cm^{-1} region. C, H and N elements were determined on a Vario EL III elemental analyzer. Thermogravimetric analyses (TGA) were performed on a Mettler TGA/SDTA851 thermal analyzer in flowing air atmosphere with a heating rate of 10 °C min^{-1} in 30–900 °C. ESR spectra were recorded at room temperature and at 77 K on a Bruker ER200-D-SRC spectrometer operating at X-band (9.4 GHz).

2.2. Synthesis of compounds *1* and *2*

2.2.1. Synthesis of $(H_2en)_{0.5}H[Cu(en)_2(H_2O)]_2\{[Cu(en)_2](\alpha_1\text{-}P_2W_{17}CuO_{61})\}\cdot 8H_2O$ (1)

A mixture of $CuCl_2\cdot 2H_2O$ (0.170 g, 1.00 mmol), K_{12}[α-$H_2P_2W_{12}O_{48}]\cdot 24H_2O$ (0.364 g, 0.09 mmol), ethylenediamine (0.05 mL, 0.74 mmol), glacial acetic acid (0.05 mL, 0.87 mmol) and H_2O (5 mL, 278 mmol) was stirred for 3 h, sealed in a 20 mL Teflon-lined stainless steel autoclave with about 25% filling, kept at 80 °C for 5 days and finally cooled to room temperature. The green lamellar crystals of **1** were filtered out, washed several times with distilled water and dried at ambient temperature. The crystals were collected mechanically. Yield: 25% based on K_{12}[α-$H_2P_2W_{12}O_{48}]\cdot 24H_2O$. Anal. calcd (%) for $C_{13}N_{13}H_{74}O_{71}Cu_4P_2W_{17}$: C, 3.13; H,1.49; N, 3.65. Found (%): C, 3.24; H, 1.65; N, 3.48.

2.2.2. Synthesis of $[4,4'\text{-}H_2bpy]_2\{[Cu(4,4'\text{-}bpy)_3][Cu(4,4'\text{-}bpy)_4(H_2O)_2]_2[Cu(4,4'\text{-}bpy)][\alpha\text{-}P_2W_{18}O_{62}]_2\}\cdot 6H_2O$ (2)

A mixture of $CuCl_2\cdot 2H_2O$ (0.085 g, 0.50 mmol), Na_{12}[α-$P_2W_{15}O_{56}]\cdot 24H_2O$ (0.216 g, 0.05 mmol), 4,4′-bpy (0.078 g, 0.50 mmol) and H_2O (5 mL, 278 mmol) was stirred for 5 h, sealed in a 20 mL teflon-lined stainless steel autoclave with about 25% filling, held at 160 °C for 5 days and finally cooled to room temperature. The cyan needle crystals of **2** were filtered, washed several times with distilled water and dried at ambient temperature. The crystals were collected mechanically. Yield: 35% based on Na_{12}[α-$P_2W_{15}O_{56}]\cdot 24H_2O$. Anal. calcd (%) for $C_{140}H_{136}$

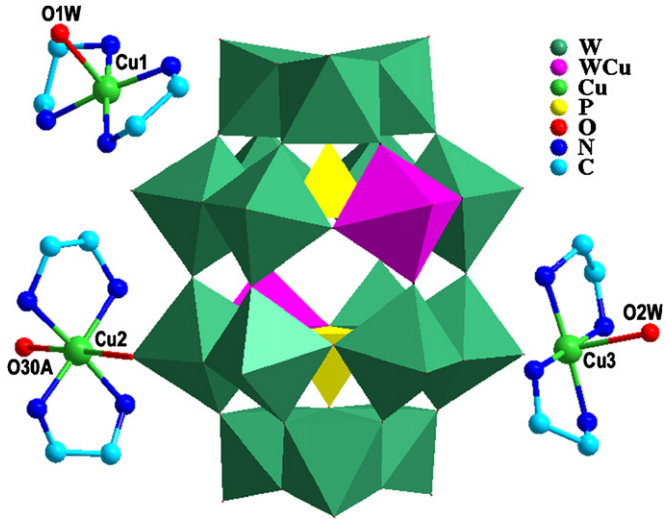

Fig. 1. The molecular structural unit of **1** with the selected atomic labeling scheme. The free diprotonated $[H_2en]^{2+}$ ion, water molecules of crystallization and hydrogen atoms are omitted for clarity. Two disordered positions in the $[\alpha_1\text{-}P_2W_{17}CuO_{61}]^{8-}$ polyoxoanion are shown in purple. The atom with "A" in the label is symmetrically generated (A: $-1+x$, y, z).

Table 1
Crystal data and structural refinement parameters for compounds **1** and **2**

	1	**2**
Empirical formula	$C_{13}H_{74}N_{13}O_{71}Cu_4P_2W_{17}$	$C_{140}H_{136}N_{28}O_{134}P_4Cu_4W_{36}$
Formula weight	4990.27	11351.41
Crystal system	Triclinic	Orthorhombic
Space group	$P-1$	$Iba2$
a (Å)	11.7626(17)	22.277(8)
b (Å)	13.246(2)	47.04(2)
c (Å)	29.350(5)	22.153(8)
α (deg)	87.355(5)	90
β (deg)	79.583(5)	90
γ (deg)	66.993(3)	90
V (Å^3)	4138.3(11)	23215(17)
Z	2	4
Dc (g cm^{-3})	4.005	3.248
μ (mm^{-1})	24.672	18.239
T (K)	293(2)	293(2)
θ (deg)	2.01–27.50	2.03–25.00
Limiting indices	$-15\leqslant h\leqslant 15$	$-26\leqslant h\leqslant 26$
	$-17\leqslant k\leqslant 17$	$-55\leqslant k\leqslant 55$
	$-38\leqslant l\leqslant 36$	$-22\leqslant l\leqslant 26$
Crystal size (mm)	$0.40\times0.07\times0.02$	$0.20\times0.07\times0.04$
Data/restrains/params	18,057/6/1056	18,812/115/1472
No. of reflns collected	31,039	72,131
No. of independent reflns	18,057	18,812
GOF on F^2	1.089	1.051
Final R indices $[I>2\sigma(I)]$[a]	$R_1=0.0563$	$R_1=0.0627$
	$wR_2=0.1505$	$wR_2=0.1477$
R indices (all data)	$R_1=0.0764$	$R_1=0.0684$
	$wR_2=0.1657$	$wR_2=0.1518$

[a] $R_1=\sum||F_o|-|F_c||/\sum|F_o|$, $wR_2=[\sum[w(F_o^2-F_c^2)^2]/\sum[w(F_o^2)^2]]^{1/2}$.

$Cu_4N_{28}O_{134}P_4W_{36}$: C, 14.81; H,1.21; N, 3.46. Found (%): C, 14.94; H, 1.31; N, 3.38.

2.3. X-ray crystallography

A single crystal with the dimensions $0.40\times0.07\times0.02\,mm^3$ for **1** and $0.20\times0.07\times0.04\,mm^3$ for **2** was glued on a glass fiber. Intensity data were collected at 293 K on a Rigaku Saturn 70 CCD diffractometer for **1** and a Rigaku Mercury 70 CCD diffractometer for **2** with graphite-monochromated Mo$K\alpha$ radiation ($\lambda=0.71703$ Å) at 293 K. Intensity data were corrected for Lorentz and polarization effects. Both structures were determined by direct methods and refined by full-matrix least-squares using the SHELXTL-97 package [41]. All hydrogen atoms were placed in idealized positions and refined with a riding model using default SHELXL parameters. Those hydrogen atoms attached to lattice water molecules were not located. In the $[\alpha_1\text{-}P_2W_{17}CuO_{61}]^{8-}$ polyoxoanion of **1**, a copper is disordered over two opposite tungsten positions (see the two positions shown in purple polyhedra in Fig. 1) and each position is occupied by half copper^{II} and half tungsten^{VI}, which leads to having one copper ion in a $[\alpha_1\text{-}P_2W_{17}CuO_{61}]^{8-}$ polyoxoanion. This disordered phenomenon is constantly encountered in POM chemistry [31,42–45]. Crystal data and structural refinement parameters

Table 2
Selected bond lengths (Å) for **1** and **2**

1		**2**	
Cu(1)–N(1)	2.009(19)	Cu(1)–N(2)^B	1.980(7)
Cu(1)–N(2)	2.027(17)	Cu(1)–N(1)	2.044(7)
Cu(1)–N(3)	2.040(17)	Cu(1)–N(3)	2.041(4)
Cu(1)–N(4)	2.04(2)	Cu(1)–N(3)^c	2.041(4)
Cu(1)–O(1W)	2.335(19)	Cu(1)–O(35)	2.488(1)
Cu(2)–N(8)	1.982(17)	Cu(1)–O(35)^c	2.488(1)
Cu(2)–N(5)	2.011(19)	Cu(2)–N(7)	2.008(5)
Cu(2)–N(7)	2.034(15)	Cu(2)–N(4)	2.034(5)
Cu(2)–N(6)	2.059(17)	Cu(2)–N(5)	2.061(5)
Cu(2)–O(52)	2.604(12)	Cu(2)–N(9)	2.058(5)
Cu(2)–O(30)^A	2.636(15)	Cu(2)–O(1W)	2.253(4)
Cu(3)–N(9)	1.99(3)	Cu(2)–O(2W)	2.919(1)
Cu(3)–N(10)	1.997(19)	Cu(3)–N(11)	1.960(7)
Cu(3)–N(12)	2.003(18)	Cu(3)–N(12)^D	2.000(7)
Cu(3)–N(11)	2.021(19)	Cu(3)–N(13)	2.042(4)
Cu(3)–O(2W)	2.52(2)	Cu(3)–N(13)^E	2.042(4)
P(1)–O(48)	1.514(13)	Cu(3)–O(11)	2.656(1)
P(1)–O(40)	1.517(12)	Cu(3)–O(11)^E	2.656(1)
P(1)–O(36)	1.536(12)	P(1)–O(28)	1.530(3)
P(1)–O(54)	1.577(12)	P(1)–O(21)	1.540(4)
P(2)–O(27)	1.512(12)	P(1)–O(16)	1.544(4)
P(2)–O(16)	1.524(11)	P(1)–O(3)	1.570(4)
P(2)–O(20)	1.550(12)	P(2)–O(37)	1.532(4)
P(2)–O(5)	1.585(12)	P(2)–O(45)	1.550(3)
		P(2)–O(51)	1.547(4)
		P(2)–O(57)	1.601(3)

Symmetry transformations used to generate equivalent atoms: A: $x-1$, y, z; B: x, $-y+1$, $z+0.5$; C: $-x+1$, $-y+1$, z; D: x, $-y+1$, $z-0.5$; E: $-x+2$, $-y+1$, z.

of **1** and **2** are presented in Table 1. Selected bond lengths (Å) for **1** and **2** are displayed in Table 2.

3. Results and discussion

3.1. Synthesis

Recently, the introduction of hydrothermal methods in the field of POMs has led to a plethora of extended materials, which are inaccessible or not easily obtainable under conventional aqueous solution conditions [13,31,46–48]. Thus, we are exploring the hydrothermal route for making such extended Dawson-based materials using lacunary POM precursors as starting materials. The successful syntheses of **1** and **2** depend on two different POM precursors under hydrothermal conditions. **1** was obtained by virtue of hexavacant $[\alpha\text{-}H_2P_2W_{12}O_{48}]^{12-}$ precursor at 80 °C while **2** was synthesized based on trivacant $[\alpha\text{-}P_2W_{15}O_{56}]^{12-}$ precursor at 160 °C. It is worth pointing out that **1** and **2** experienced the transformation between different lacunary polyoxoanions. In the formation of **1**, the transformation of hexavacant $[\alpha\text{-}H_2P_2W_{12}O_{48}]^{12-}$ → monovacant $[\alpha_1\text{-}P_2W_{17}O_{61}]^{10-}$ must have happened. In fact, Contant [40] has systematically studied the transformations between different lacunary Dawson phosphotungstate anions and observed that $[\alpha\text{-}H_2P_2W_{12}O_{48}]^{12-}$ could be isomerized to $[\alpha_1\text{-}P_2W_{17}O_{61}]^{10-}$ under the acidic condition. Recently, Pope et al. reported that $[P_8W_{48}O_{184}]^{40-}$ could be transformed into $[\alpha_2\text{-}P_2W_{17}O_{61}]^{10-}$ at higher pH value while it could be transformed into $[\alpha\text{-}P_2W_{18}O_{62}]^{6-}$ at lower pH value [49]. It should be noted that **2** contains plenary $[\alpha\text{-}P_2W_{18}O_{62}]^{6-}$ polyoxoanions, although the reaction was carried out using trivacant $[\alpha\text{-}P_2W_{15}O_{56}]^{12-}$ polyoxoanion as the starting material. The phenomena that the plenary $[\alpha\text{-}P_2W_{18}O_{62}]^{6-}$ polyoxoanion loses tungsten atoms in the reaction have been previously observed. For example, the $[\alpha\text{-}P_2W_{18}O_{62}]^{6-}$ polyoxoanion can be degraded into the $[\alpha\text{-}P_2W_{15}O_{56}]^{12-}$ polyoxoanion under the basic condition [40]. In contrast, the phenomena that the trivacant $[\alpha\text{-}P_2W_{15}O_{56}]^{12-}$ polyoxoanion obtains tungsten atoms in the reaction have been also observed in our exploring the reaction of $[\alpha\text{-}P_2W_{15}O_{56}]^{12-}$ polyoxoanions with Cu^{2+} ions. For instance, we found the transformation of $[\alpha\text{-}P_2W_{15}O_{56}]^{12-}$ → $[\alpha_1\text{-}P_2W_{17}O_{61}]^{10-}$ in the formation of $[Cu(en)_2(OH_2)]\{[Cu(en)_2]_2[Cu(en)_2\text{-}(OH_2)][Cu(en)][\alpha_1\text{-}P_2W_{17}CuO_{61}]\}\cdot 3H_2O$. Many experimental results have proved that both $[\alpha\text{-}P_2W_{18}O_{62}]^{6-}$ and $[\alpha\text{-}P_2W_{15}O_{56}]^{12-}$ polyoxoanions can be mutually transformed under the basic or acidic conditions [50]. Notice that **1** and **2** cannot be synthesized by $[\alpha_1\text{-}P_2W_{17}O_{61}]^{10-}$ and $[\alpha\text{-}P_2W_{18}O_{62}]^{6-}$ precursors, respectively, under hydrothermal conditions.

3.2. Structural description

Compound **1** consists of a 1-D linear chain structure constructed from monocopper^{II}-substituted Dawson $[\alpha_1\text{-}P_2W_{17}CuO_{61}]^{8-}$ polyoxoanions while **2** exhibits a novel 2-D extended structure containing plenary Dawson $[\alpha\text{-}P_2W_{18}O_{62}]^{6-}$ polyoxoanions. The $[\alpha_1\text{-}P_2W_{17}CuO_{61}]^{8-}$ polyoxoanion can be viewed as a derivative of the parent $[\alpha\text{-}P_2W_{18}O_{62}]^{6-}$ polyoxoanion by removal of a belt $W{=}O_t$ group and then inhabited by a Cu^{II} atom. The parent $[\alpha\text{-}P_2W_{18}O_{62}]^{6-}$ polyoxoanion with a virtual D_{3h} symmetry can be described as a fusion product of a couple of $[\alpha\text{-}PW_9O_{31}]^{3-}$ units derived from the well-known α-Keggin $[\alpha\text{-}PW_{12}O_{40}]^{3-}$ polyoxoanion by removal of a set of three corner-sharing WO_6 octahedra [31,32]. In $[\alpha_1\text{-}P_2W_{17}CuO_{61}]^{8-}$ in **1** and $[\alpha\text{-}P_2W_{18}O_{62}]^{6-}$ in **2**, the *M*–O (*M* = W^{VI} or Cu^{II}) distances can be divided into four groups according to the numbers and types of oxygen atoms: (1) There are 17 for **1** and 18 for **2** terminal O atoms which are only bonded to one *M* atom, the *M*–O distances vary from 1.699(13) to 2.036(16) Å for **1** and 1.671(4) to 1.741(5) Å for **2**. (2) There are 36 O atoms which are shared by two *M* atoms. The *M*–O distances range from 1.815(11) to 2.016(13) Å for **1** and 1.823(5) to 2.014(4) Å for **2**. (3) There are 6 O atoms which are combined with one P atom and two *M* atoms. The *M*–O distances are between 2.299(12) and 2.384(11) Å for **1** and between 2.318(3) and 2.402(3) Å for **2**. (4) There are 2 O atoms which are coordinated to one P atom and three W atoms. The W–O distances are in the range of 2.366(10)–2.400(11) Å for **1** and 2.355(3)–2.420(4) Å for **2**. Except for *M*–O bond lengths related to two disordered positions in **1**, these bond lengths are within the normal ranges and in close agreement with those described in the literatures [27,29]. The *M*–O distances related to two disordered positions (labeled as W17 and W18) in **1** are in the range of 1.887(12)–2.387(12) Å for W17 and 1.923(11)–2.406(13) Å for W18, respectively, which further confirms that two disordered positions are simultaneously occupied by the Cu^{II} and W^{VI} elements.

Compound **1** crystallizes in the triclinic space group *P*−1. The formula unit consists of one monocopper^{II}-substituted Dawson $[\alpha_1\text{-}P_2W_{17}CuO_{61}]^{8-}$ polyoxoanion, one $[Cu(en)_2]^{2+}$ cation, two $[Cu(en)_2(H_2O)]^{2+}$ cations, a half discrete $[H_2en]^{2+}$ ion, one proton and eight lattice water molecules (Fig. 1). It should be noted that **1** is somewhat different from $[Cu(en)_2(OH_2)]_2[H_2en][\{Cu(en)_2\}P_2CuW_{17}O_{61}]\cdot 5H_2O$ (**3**) [31] and $[Cu(en)_2(OH_2)]_2[Cu(en)_2]_{0.5}[H_2en]_{0.5}[\{Cu(en)_2\}P_2CuW_{17}O_{61}]\cdot 5H_2O$ (**4**) [31] though they all contain the 1-D chain structures with the same connection motif. Comparing **1** with **3**, the most obvious discrepancy between them is that their cell constants are completely distinct: **1** crystallizes in the triclinic space group *P*−1 with $a = 11.7626(17)$, $b = 13.246(2)$, $c = 29.350(5)$ Å, $\alpha = 87.355(5)$, $\beta = 79.583(5)$, $\gamma = 66.993(3)^\circ$ and $V = 4138.3(11)$ Å^3; whereas **3** belongs to the triclinic space group *P*−1, $a = 11.710(4)$, $b = 13.228(4)$, $c = 28.161(8)$ Å, $\alpha = 90.58(2)$, $\beta = 95.76(2)$, $\gamma = 112.52(2)^\circ$ and $V = 4004(2)$ Å^3. Comparing **1** with **4**, although both have similar cell constants (triclinic, *P*−1, $a = 11.724(3)$, $b = 13.239(3)$, $c = 29.571(6)$ Å, $\alpha = 89.30(1)$, $\beta = 79.36(1)$, $\gamma = 66.70(1)^\circ$, $V = 4134(2)$ Å^3 for **4**), the type of the charge balance

cations and the number of lattice water molecules are different: there are 1 $[Cu(en)_2]^{2+}$, 2 $[Cu(en)_2(H_2O)]^{2+}$, 0.5 $[H_2en]^{2+}$, 1 H^+ and 8 lattice water molecules in **1** while there are 1.5 $[Cu(en)_2]^{2+}$, 2 $[Cu(en)_2(H_2O)]^{2+}$, 0.5 $[H_2en]^{2+}$ and 5 lattice water molecules in **4**. From the aforementioned analysis, because in **1** there exist 1 H^+ charge countercation rather than 0.5 $[Cu(en)_2]^{2+}$ cation and 8 rather than 5 lattice water molecules, these differences directly lead to the difference of the α angle ($\alpha = 87.355(5)^\circ$ for **1** and $\alpha = 89.30(1)^\circ$ for **4**). As a result, albeit both structures contain the 1-D chain structures with the same connection motif, **1** and **4** are crystallographically and chemically different. Furthermore, the synthetic conditions of **1** and **4** are quite distinct: **1** was prepared by the hydrothermal reaction of a mixture of $CuCl_2 \cdot 2H_2O$ (0.170 g), $K_{12}[\alpha\text{-}H_2P_2W_{12}O_{48}] \cdot 24H_2O$ (0.364 g), en (0.05 mL), glacial acetic acid (0.05 mL) and H_2O (5 mL, 278 mmol) at 80 °C for 5 days, in contrast, **4** was made by the hydrothermal reaction of NaF (0.2 g), $Cu(NO)_3 \cdot 3H_2O$ (0.26 g), en (1.5 g), $Na_2WO_4 \cdot 2H_2O$ (1.50 g), H_3PO_4 (0.78 g, 85%) and H_2O (20 mL) at 140 °C for 18 days. In addition, since **1** was synthesized under the acidic conditions, it is common that one proton can be used to act as the charge balance cation. Moreover, this phenomenon is constantly encountered in POM chemistry [17,51,52]. Adjacent $[\alpha_1\text{-}P_2W_{17}CuO_{61}]^{8-}$ polyoxoanions are interconnected through a common bridging oxygen atom and a bridging $[Cu2(en)_2]^{2+}$ cation to generate an infinite 1-D linear chain parallel to the α-axis (Fig. 2). The bridging oxygen atom connects two opposite positions of the Dawson polyoxoanion occupied by Cu^{II} and W^{VI} with the occupancy of one half. This situation is similar to those in **3** [31], **4** [31] and $[ET]_8[PW_{11}MnO_{39}] \cdot 2H_2O$ [44]. In $[ET]_8[PW_{11}MnO_{39}] \cdot 2H_2O$ [44], the two positions linking to the bridging oxygen atom are occupied by Mn^{II} and W^{VI} with an occupancy of one half. It should be noted that the two disordered sites are in the "belt" positions of the $[\alpha_1\text{-}P_2W_{17}CuO_{61}]^{8-}$ polyoxoanion in **1**. This is different from $[Me_2NH_2]_8[P_2W_{17}CoO_{61}] \cdot 11H_2O$, in which a cobalt atom occupies a "cap" position of the $[P_2W_{17}CoO_{61}]^{8-}$ polyoxoanion [53]. To the best of our knowledge, this chain architecture mode by a common bridging oxygen atom and a bridging $[Cu2(en)_2]^{2+}$ cation in **1** is very rare in POM chemistry and similar to those observed in **3** [31], **4** [31] and $[\{Cu(en)_2\}_3(\alpha\text{-}PW_{11}CuO_{39}Cl)] \cdot 6H_2O$ [54]. The two discrete $[Cu1(en)_2(H_2O)]^{2+}$ and $[Cu3(en)_2(H_2O)]^{2+}$ cations adopt a five-coordinate square pyramidal geometry defined by four nitrogen atoms from two en ligands and one water oxygen atom [Cu–N: 1.99(3)–2.04(2) Å and Cu–O: 2.335(19)–2.52(2) Å]. The $[Cu2(en)_2]^{2+}$ cation employs an six-coordinate octahedral configuration built by four nitrogen atoms from two en ligands and two terminal oxygen atoms from two $[\alpha_1\text{-}P_2W_{17}CuO_{61}]^{8-}$ polyoxoanions [Cu–N: 1.982(17)–2.059(17) Å and Cu–O: 2.604(12)–2.636(15) Å]. The bond valence sum (BVS) calculations are performed to identify the oxidation states of the copper ions in **1** and **2**. The BVS values of Cu1, Cu2 and Cu3 ions in **1** and **2** are 1.76, 1.75 and 1.77 for **1** and 1.79, 1.74 and 1.78 for **2**, respectively, revealing that the oxidation state of each copper ion is +2. These results are in good consistence with their square pyramidal and octahedral coordination geometries.

Compound **2** crystallizes in the orthorhombic space group *Iba*2. Structural analysis indicates that the molecular structural unit of **2** is composed of one $[Cu(1)(4,4'\text{-bpy})]^{2+}$ cation, two $[Cu(2)(4,4'\text{-bpy})_4(H_2O)_2]^{2+}$ cations, one $[Cu(3)(4,4'\text{-bpy})_3]^{2+}$ cation, two $[\alpha\text{-}P_2W_{18}O_{62}]^{6-}$ polyoxoanions, two discrete diprotonated $[4,4'\text{-}H_2bpy]^{2+}$ ions and six lattice water molecules (Fig. 3). In **2**, there are three crystallographically unique copper ions (Cu1, Cu2 and Cu3), each of which plays different special roles in the construction of the 2-D extended structure. The weak long Cu–O interactions will be considered because the evident Jahn-Teller effect of the $copper^{II}$ ion in the crystal field leads to the elongation of Cu–O distances [54–57]. The $[Cu(1)(4,4'\text{-bpy})]^{2+}$ cation is six-coordinate octahedral geometry defined by four nitrogen atoms from four 4,4′-bpy ligands and two terminal oxygen atoms from two $[\alpha\text{-}P_2W_{18}O_{62}]^{6-}$ polyoxoanions. The Cu–N and Cu–O distances are in the range of 1.980(7)–2.044(7) Å and 2.488(1) Å, respectively. The $[Cu(2)(4,4'\text{-bpy})_4(H_2O)_2]^{2+}$

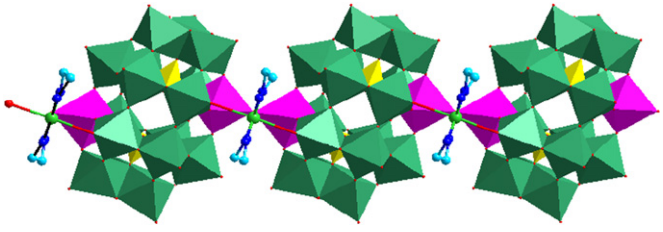

Fig. 2. The infinite 1-D linear chain parallel to the *a* axis in **1** constructed from monocopper-substituted Dawson polyoxoanions $[\alpha_1\text{-}P_2W_{17}CuO_{61}]^{8-}$ through common bridging oxygen atoms and bridging $[Cu2(en)_2]^{2+}$ cations. Two disordered positions in the $[\alpha_1\text{-}P_2W_{17}CuO_{61}]^{8-}$ polyoxoanion are shown in purple.

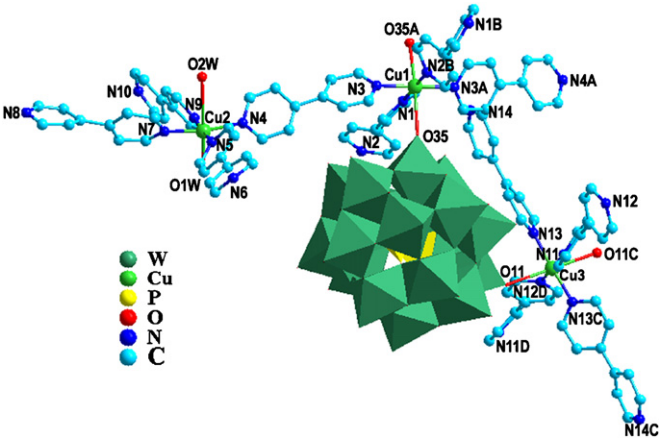

Fig. 3. The asymmetric unit of **2** with the selected atomic labeling scheme. The free diprotonated $[4,4'\text{-}H_2bpy]^{2+}$ ion, water molecules of crystallization and hydrogen atoms are omitted for clarity. Atoms with "A–D" in their labels are symmetrically generated (A: $1-x$, $1-y$, z; B: $1-x$, y, $0.5+z$; C: $2-x$, $1-y$, z; D: $2-x$, y, $-0.5+z$).

cation is also six-coordinate octahedral geometry defined by four nitrogen atoms from four 4,4′-bpy ligands and two water oxygen atoms [Cu–N: 2.008(5)–2.061(5) Å and Cu–O: 2.253(4)–2.919(1) Å]. The coordination environment of the $[Cu(3)(4,4'\text{-bpy})_3]^{2+}$ cation [Cu–N: 1.960(7)–2.042(4) Å and Cu–O: 2.656(1) Å] is similar to that of the $[Cu(1)(4,4'\text{-bpy})]^{2+}$ cation. It is of interest that each $[\alpha\text{-}P_2W_{18}O_{62}]^{6-}$ polyoxoanion acts as a bidendate ligand to combine one $[Cu(3)(4,4'\text{-bpy})_3]^{2+}$ cation with one $[Cu(1)(4,4'\text{-bpy})]^{2+}$ cation in **2**.

It is noteworthy that Cu1 ions construct a 1-D linear cationic chain $[Cu(1)(4,4'\text{-bpy})]_n^{2n+}$ by the bridging role of 4,4′-bpy ligands. Similar 1-D linear cationic chains formed by copper ions and 4,4′-bpy ligands have been seen previously in several Keggin-based [17,23,58] and one Dawson-based [29] POMs. For example, in $[Cu^{I}(4,4'\text{-bpy})]_3[PMo_{10}^{VI}Mo_2^{V}O_{40}\{Cu^{II}(2,2'\text{-bpy})\}]$, the monocopper-capped Keggin polyoxoanions $[PMo_{10}^{VI}Mo_2^{V}O_{40}\{Cu^{II}(2,2'\text{-bpy})\}]^{3-}$ are linked by the 1-D linear cationic chains $[Cu^{I}(4,4'\text{-bpy})]_n^{n+}$ to construct a 2-D network [58]. For **2**, a couple of $[\alpha\text{-}P_2W_{18}O_{62}]^{6-}$ polyoxoanions in a staggered pattern join to the Cu1 ion via a terminal oxygen atom in both sides of each Cu1 ion (Fig. 4). Two symmetrically related $[Cu(2)(4,4'\text{-bpy})_4(H_2O)_2]^{2+}$ cations link to a $[Cu(1)(4,4'\text{-bpy})]^{2+}$ cation via two rigid 4,4′-bpy bridges (Fig. 5). The architecture fashion of the Cu3 ions is very similar to that of the Cu1 ions and also form a 1-D linear cationic chain $[Cu3(4,4'\text{-bpy})]_n^{2n+}$ through the 4,4′-bpy ligands. More fascinatingly, the most striking structural feature is that $[\alpha\text{-}P_2W_{18}O_{62}]^{6-}$ polyoxoanions function as bidendate ligands to connect adjacent $[Cu1(4,4'\text{-bpy})]_n^{2n+}$ and $[Cu3(4,4'\text{-bpy})]_n^{2n+}$ linear cationic chains together constructing a 2-D extended structure (Fig. 6). Although a 2-D inorganic–organic hybrid $(NH_4)_3(4,4'\text{-}H_2bpy)[Cu^{I}(4,4'\text{-bpy})]_7[P_2W_{18}O_{62}]_2\cdot 10H_2O$ built by saturated Dawson-type polyoxoanions and copper(*I*)-4,4′-bpy cations has been recently reported [29], **2** still represents the first 2-D inorganic–organic hybrid POM constructed from saturated Dawson-type polyoxoanions and copper(II)-4,4′-bpy cations. Topologically, the 2-D extended structure of **2** can be simplified to a bimodal 4-connected net. In this simplification, Cu1 atoms act as one kind of the 4-connected nodes and Cu3 atoms function as the other kind of the 4-connected nodes. The ratio of two kinds of nodes is 1:1. By a close insight into the arrangement of adjacent 4-connected topological sheets, the distribution of sheets is in the –ABAB– arrangement mode and the spacing of the interlayers is ca. 26.0 Å (Fig. 7). The void gaps between sheets are filled with 4,4′-bpy and lattice water molecules. Interestingly, the $[\alpha\text{-}P_2W_{18}O_{62}]^{6-}$, Cu1 and Cu3 ions arrange in the helical distribution motif along the [100] direction generating the helical chain structures. Adjacent two helical chains have

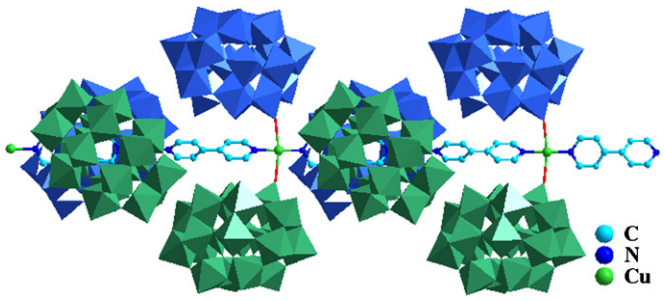

Fig. 4. The connection motif of the linear $[Cu1(4,4'\text{-bpy})]_n^{2n+}$ chain and $[\alpha\text{-}P_2W_{18}O_{62}]^{6-}$ polyoxoanions. The blue and green $[\alpha\text{-}P_2W_{18}O_{62}]^{6-}$ polyoxoanions highlight the staggered pattern. The $[Cu(2)(4,4'\text{-bpy})_4(H_2O)_2]^{2+}$ cations linking to the $[Cu1(4,4'\text{-bpy})]_n^{2n+}$ chain are omitted for clarity.

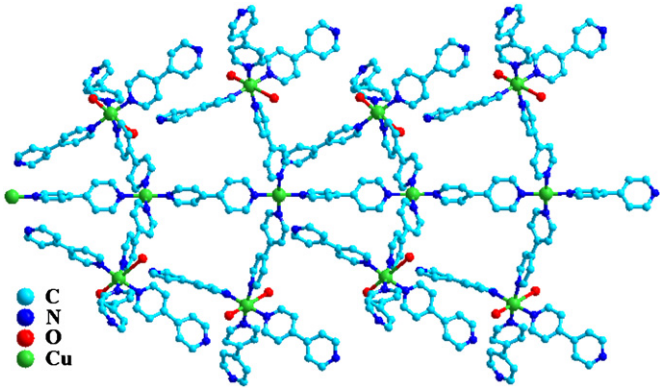

Fig. 5. The connection motif of the linear $[Cu1(4,4'\text{-bpy})]_n^{2n+}$ chain and $[Cu(2)(4,4'\text{-bpy})_4(H_2O)_2]^{2+}$ cations. The $[\alpha\text{-}P_2W_{18}O_{62}]^{6-}$ polyoxoanions linking to the $[Cu1(4,4'\text{-bpy})]_n^{2n+}$ chain are omitted for clarity.

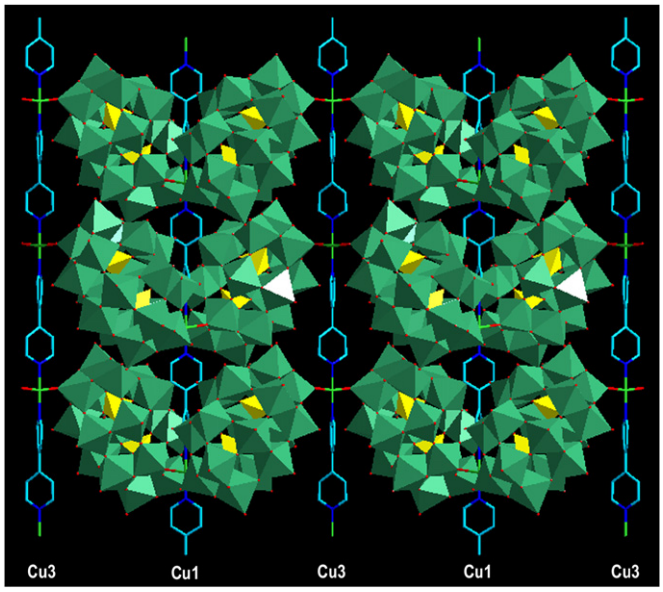

Fig. 6. The 2-D structure constructed from $[Cu1(4,4'\text{-bpy})]_n^{2n+}$, $[Cu3(4,4'\text{-bpy})]_n^{2n+}$ chains and $[\alpha\text{-}P_2W_{18}O_{62}]^{6-}$ polyoxoanions. The Cu1 and Cu3 symbols represent $[Cu1(4,4'\text{-bpy})]_n^{2n+}$ and $[Cu3(4,4'\text{-bpy})]_n^{2n+}$ chains, respectively. The monodendate 4,4′-bipy ligands on Cu1 and Cu3 cations are omitted for clarity.

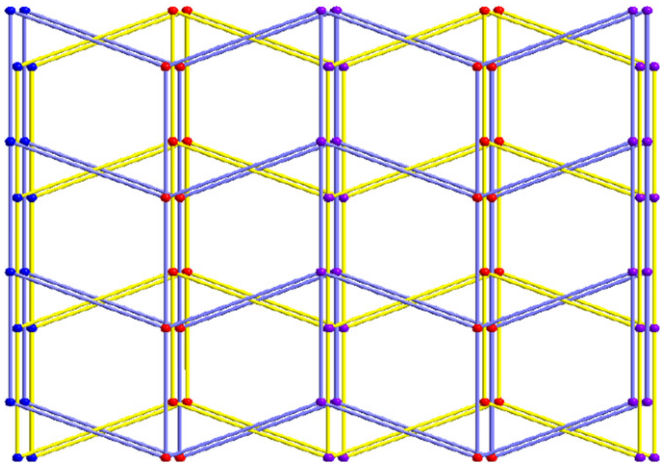

Fig. 7. The –ABAB– packing mode of the 4-connected topological sheets. The blue and red balls represent Cu3 and Cu1 nodes, respectively.

the opposite handedness (Fig. 8). Similar phenomenon is very rare in the POM chemistry [34,39,59].

Though both **2** and $(NH_4)_3(4,4'\text{-}H_2bpy)[Cu^I(4,4'\text{-}bpy)]_7[P_2W_{18}O_{62}]_2\cdot 10H_2O$ [29] employ the inorganic–organic hybrid 2-D extended structure, seven obvious differences in structure are present owing to their different construction modes and crystallographic symmetries: (a) The former crystallizes in the orthorhombic space group *Iba*2 whereas the latter belongs to the triclinic space group $P\bar{1}$. (b) There are three crystallographically unique Cu^{2+} ions in the former while four crystallographically unique Cu^{+} ions exist in the latter. (c) All the Cu^{2+} ions in the former are six-coordinate octahedral geometry while the coordination geometries of the Cu^{+} ions in the latter have three types (two-coordinate linear geometry, three-coordinate T-shaped geometry and four-coordinate tetrahedral geometry). (d) Two types of Cu^{2+} ions (Cu1 and Cu3) participate in the construction of two 1-D linear cationic chains $[Cu(4,4'\text{-bpy})]_n^{2n+}$ in the former while three types of Cu^{+} ions (Cu2, Cu3 and Cu4) take part in the formation of three 1-D linear cationic chains $[Cu(4,4'\text{-bpy})]_n^{n+}$ in the latter. (e) The $[\alpha\text{-}P_2W_{18}O_{62}]^{6-}$ polyoxoanion acts as a bidendate ligand in the former whereas a tetradendate one in the latter. (f) From the topological point of view, the 2-D structure of the former belongs to the (4,4)-connected topological network, in contrast, the 2-D structure of the latter is the (3,4)-connected topological network. (g) The arrangements of the $[\alpha\text{-}P_2W_{18}O_{62}]^{6-}$, Cu1 and Cu3 ions along the [001] direction in the former result in the helical chains with the opposite handedness, however, there is no helical chain in the latter.

3.3. IR spectra

In the IR spectra of **1** and **2**, there are four characteristic asymmetric vibration bands resulting from the Dawson-type polyoxoanion, namely, $\nu_{as}(W{=}O_t)$, $\nu_{as}(W\text{–}O_b)$, $\nu_{as}(W\text{–}O_c)$ and $\nu_{as}(P\text{–}O_a)$. Comparing to the IR spectra of **2** and $\alpha\text{-}H_6P_2W_{18}O_{62}\cdot nH_2O$ [27], the P–O vibration band and the

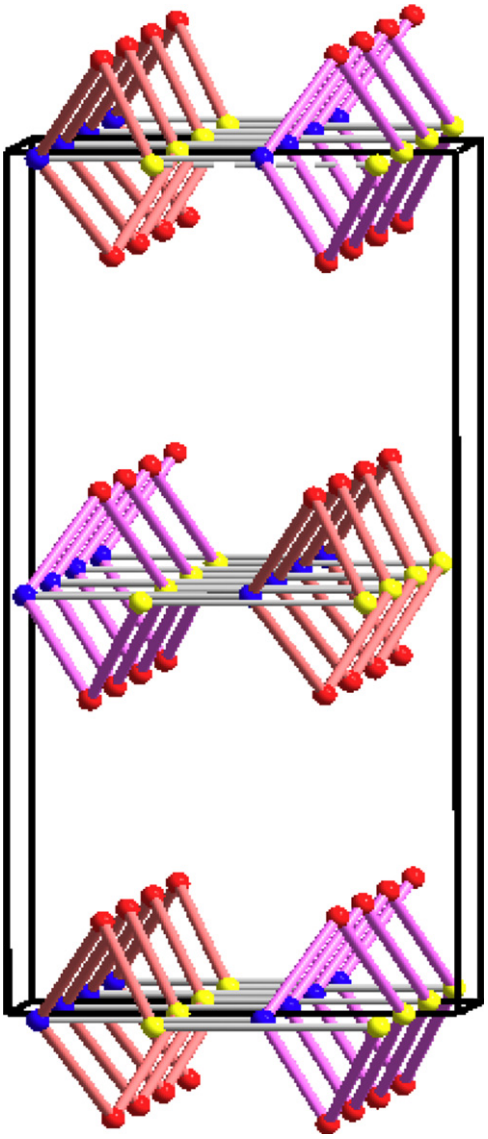

Fig. 8. The arrangement of the helical chains built by the $[\alpha\text{-}P_2W_{18}O_{62}]^{6-}$, Cu1 and Cu3 ions along the [100] direction in a unit cell and adjacent two helical chains having the opposite handedness. The blue, yellow and red balls represent Cu1, Cu3 and $[\alpha\text{-}P_2W_{18}O_{62}]^{6-}$ moieties, respectively.

W–O_c vibration band in **1** both split into three bands, namely, $\nu_{as}(P\text{–}O_a)$: 1124, 1080 and 1040 cm^{-1}; $\nu_{as}(W\text{–}O_c)$: 798, 770 and 746 cm^{-1}. This splitting of vibration bands is related to the lower symmetry of the $[\alpha_1\text{-}P_2W_{17}CuO_{61}]^{8-}$ polyoxoanion resulting from the encapsulation of a Cu^{II} ion into the vacant site of the $[\alpha_1\text{-}P_2W_{17}O_{61}]^{10-}$ polyoxoanion. In addition, the $W{=}O_t$ and $W\text{–}O_b$ vibration bands appear at 943 and 903 cm^{-1}, respectively. The stretching bands of the $–NH_2$ and $–CH_2$ groups are observed at 3320–3250 cm^{-1} and 3050–2950 cm^{-1} are indicative of the presence of en in **1**. Comparing the IR spectrum of **2** to that of $\alpha\text{-}H_6P_2W_{18}O_{62}\cdot nH_2O$ [27], the $W{=}O_t$ vibration band has a red-shift from 961 to 955 cm^{-1}, the $W\text{–}O_b$ vibration band also has a red-shift from 913 to 903 cm^{-1}, while the W–O_c vibration band has a blue-shift from 780 to 786 cm^{-1}. The P–O_a vibration band appears nearly identical to that of the

parent acid α-$H_6P_2W_{18}O_{62}\cdot nH_2O$ [27]. These results indicate that the polyoxoanions in **2** are some distorted due to the coordination effects of copper^{II}-4,4′-bpy cations [6,26], which are confirmed by the result of the crystal structure. The vibration peaks between 1600 and 1400 cm^{-1} are indicative of the presence of the 4,4′-bipy group in **2**. The phenomena of red-/blue-shifts of the characteristic vibration bands of **1** and **2** display strong interactions between the polyoxoanions and copper-organic complexes in the solid state.

3.4. Thermogravimetric analysis

Compounds **1** and **2** undergo a two-step loss weight process from 30 to 900 °C (Fig. 9). For **1**, the weight loss of 2.83% during the first step from 30 to 282 °C involves the loss of 8 lattice water molecules (calcd 2.88%). On further heating, the second weight loss is 9.27% between 282 and 900 °C, corresponding to the removal of 0.5 diprotonated $[H_2en]^{2+}$ ion, 6 coordinated en ligands and 2 coordinated water molecules and the dehydration of 1 proton (calcd 8.88%). For **2**, the first weight loss is 1.04% in the range of 30–121 °C, corresponding to the loss of 6 lattice water molecules (calcd 0.95%). The second weight loss of 19.95% between 121 and 900 °C is attributed to the removal of 4 coordinated water molecules, 2 diprotonated $[4,4'\text{-}H_2bpy]^{2+}$ ions and 14 coordinated 4,4′-bpy ligands (calcd 20.22%). The observed experimental values are in excellent consistence with the theoretical values.

3.5. Electron spin resonance (ESR) spectra

X-band powder ESR spectra of **2** recorded at room temperature and 77 K are depicted in Fig. 10. At room temperature, the ESR spectrum displays an anisotropic broad resonance at ca. 3400 G with the line width $\Delta H_{PP} = 900$ G. When the temperature is lowered to 77 K, the intensity of this spectrum somewhat increases and stays at $g = 2.15$, indicative of the presence of the expected copper^{II} ion in **2** [60]. The principal value of the g tensor is typical of the copper^{II} ions in the octahedral environment with the unpaired electron on the d_{x2-y2} orbital. The line width ΔH_{PP} remains unchanged at room temperature and 77 K, indicating that the spin–spin relaxation process competes and is comparable to the magnitude order of the spin–lattice relaxation process. These indicate an overall relaxation time almost is temperature independent [61].

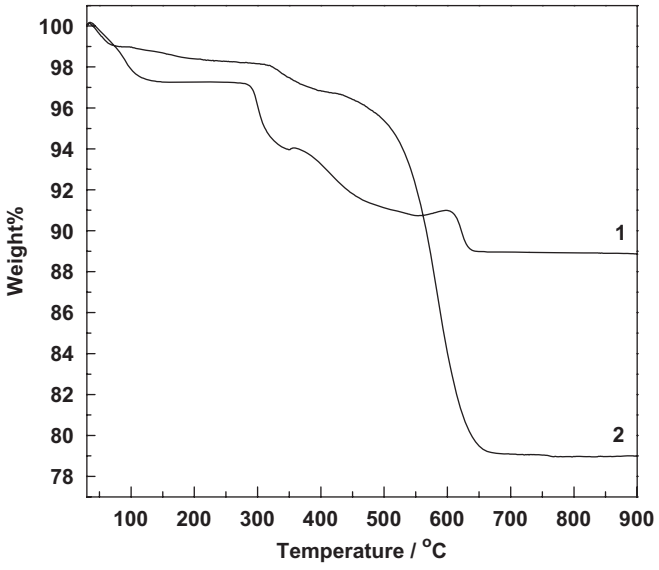

Fig. 9. The TGA curves of **1** and **2** measured in flowing air atmosphere with a heating rate of 10 °C min^{-1} in 30–900 °C.

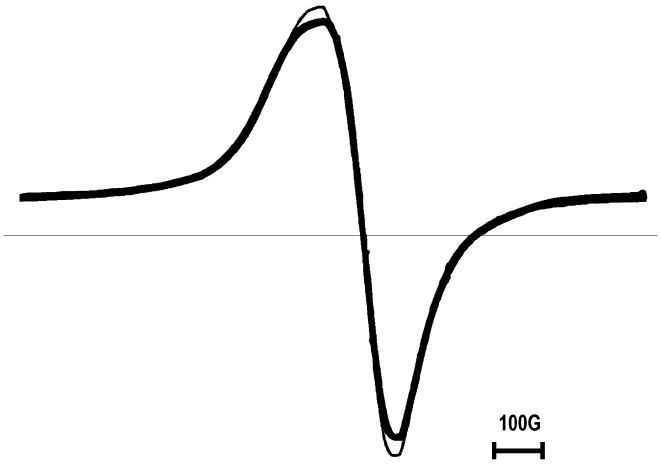

Fig. 10. X-band powder ESR spectra of **2** recorded at room temperature and 77 K. The thick and thin solid lines represent the room temperature and 77 K spectral lines, respectively.

4. Conclusion

Two Dawson-based phosphotungstates $(H_2en)_{0.5}H[Cu(en)_2(H_2O)]_2\{[Cu(en)_2](\alpha_1\text{-}P_2W_{17}CuO_{61})\}\cdot 8H_2O$ (1) and $[4,4'\text{-}H_2bpy]_2\{[Cu(4,4'\text{-}bpy)_3][Cu(4,4'\text{-}bpy)_4(H_2O)_2]_2[Cu(4,4'\text{-}bpy)][\alpha\text{-}P_2W_{18}O_{62}]_2\}\cdot 6H_2O$ (2) have been hydrothermally synthesized and structurally characterized by IR spectra, elemental analysis, TGA and single-crystal X-ray diffraction. **1** contains a 1-D linear chain constructed from monocopper^{II}-substituted Dawson polyoxoanions $[\alpha_1\text{-}P_2W_{17}CuO_{61}]^{8-}$, while **2** represents the first 2-D sheet-like structure with a (4,4)-connected topological net built up from plenary Dawson-type polyoxoanions and Cu^{II}-4,4′-bpy cations in the POM chemistry.

Acknowledgments

The authors are thankful for the financial supports from the National Natural Science Fund for Distinguished Young Scholars of China (No. 20725101), the 973 program (No. 2006CB932904), the NSF of Fujian Province (No. E0510030) and the Knowledge Innovation Program from CAS (No. KJCX2.YW.H01).

Appendix A. Supplementary materials

CCDC 658565 and 658566 for **1** and **2** contain the crystallographic data for this paper. These data can be obtained free of charge via www.ccdc.cam.ac.uk/data_request/cif or from the Cambridge Crystallographic Data Center, 12 Union Road, Cambridge CB2 1EZ, UK (Fax: +44 1223 336033; e-mail: deposit@ccdc.cam.ac.uk).

References

[1] J.T. Rhule, W.A. Neiwert, K.I. Hardcastle, B.T. Do, C.L. Hill, J. Am. Chem. Soc. 123 (2001) 12101–12102.
[2] M.L. Wei, C. He, W.J. Hua, C.Y. Duan, S.H. Li, Q.J. Meng, J. Am. Chem. Soc. 128 (2006) 13318–13319.
[3] Z. Han, Y. Zhao, J. Peng, E. Wang, Eur. J. Inorg. Chem. (2005) 264–271.
[4] R.C. Finn, R.S. Rarig Jr., J. Zubieta, Inorg. Chem. 41 (2002) 2109–2123.
[5] S.T. Zheng, J. Zhang, G.Y. Yang, Inorg. Chem. 44 (2005) 2426–2430.
[6] J. Niu, D. Guo, J. Wang, J. Zhao, Cryst. Growth Des. 4 (2004) 241–247.
[7] H. An, Y. Li, E. Wang, Inorg. Chem. 44 (2005) 6062–6070.
[8] P.J. Hagrman, D. Hagrman, J. Zubieta, Angew. Chem. Int. Ed. 38 (1999) 2638–2684.
[9] U. Kortz, M.G. Savelieff, F.Y. Abou-Ghali, L.M. Khalil, S.A. Maalouf, D.I. Sinno, Angew. Chem. Int. Ed. 41 (2002) 4070–4073.
[10] X. Huang, J. Li, H. Fu, J. Am. Chem. Soc. 122 (2000) 8789–8790.
[11] C. Wu, C. Lu, X. Lin, D. Wu, S. Lu, H. Zhuang, J. Huang, Chem. Commun. (2003) 1284–1285.
[12] C. Liu, Y. Hou, J. Zhang, S. Gao, Inorg. Chem. 41 (2002) 140–143.
[13] Y.P. Ren, X.J. Kong, X.Y. Hu, M. Sun, L.S. Long, R.S. Huang, L.S. Zheng, Inorg. Chem. 45 (2006) 4016–4023.
[14] A. Mueller, W. Plass, E. Krickemeyer, S. Dillinger, H. Bögge, A. Armatage, A. Proust, C. Beugholt, U. Bergmann, Angew. Chem. Int. Ed. Engl. 33 (1994) 849–851.
[15] M. Yaun, Y. Li, E. Wang, C. Tian, L. Wang, N. Hu, H. Jia, Inorg. Chem. 42 (2003) 3670–3676.
[16] Y. Xu, J.Q. Xu, K. Zhang, Y. Zhang, X. You, Chem. Commun. (2000) 153–154.
[17] Y. Lu, Y. Xu, E. Wang, J. Lü, C. Hu, L. Xu, Cryst. Growth Des. 5 (2005) 257–260.
[18] J. Niu, Q. Wu, J. Wang, J. Chem. Soc. Dalton Trans. (2002) 2512–2516.
[19] E. Burkholder, V. Golub, C.J. O'Connor, J. Zubieta, Inorg. Chem. Commun. 7 (2004) 363–366.
[20] C. Lei, J.G. Mao, Y.Q. Sun, J.L. Song, Inorg. Chem. 43 (2004) 1964–1968.
[21] P.Q. Zheng, Y.P. Ren, L.S. Long, R.B. Huang, L.S. Zheng, Inorg. Chem. 44 (2005) 1190–1192.
[22] H. Jin, C. Qin, Y. Li, E. Wang, Inorg. Chem. Commun. 9 (2006) 482–485.
[23] J. Sha, J. Peng, H. Liu, J. Chen, B. Dong, A. Tian, Z. Su, Eur. J. Inorg. Chem. (2007) 1268–1274.
[24] J. Chen, T. Lan, Y. Huang, C. Wei, Z. Li, Z. Zhang, J. Solid State Chem. 179 (2006) 1904–1910.
[25] X.J. Kong, Y.P. Ren, P.Q. Zheng, Y.X. Long, L.S. Long, R.B. Huang, L.S. Zheng, Inorg. Chem. 45 (2006) 10702–10711.
[26] J. Niu, D. Guo, J. Zhao, J. Wang, New J. Chem. 28 (2004) 980–987.
[27] J. Wang, J. Zhao, J. Niu, J. Mol. Struct. 697 (2004) 191–198.
[28] T. Soumahoro, E. Burkholder, W. Ouellette, J. Zubieta, Inorg. Chim. Acta. 358 (2005) 606–616.
[29] H. Jin, Y. Qi, D. Xiao, X. Wang, S. Chang, E. Wang, J. Mol. Struct. 837 (2007) 23–29.
[30] A. Tian, Z. Han, J. Peng, B. Dong, J. Sha, B. Li, J. Mol. Struct. 832 (2007) 117–123.
[31] B. Yan, Y. Xu, X. Bu, N.K. Goh, L.S. Chia, G.D. Stucky, J. Chem. Soc. Dalton Trans. (2001) 2009–2014.
[32] Y. Lu, Y. Xu, Y. Li, E. Wang, X. Xu, Y. Ma, Inorg. Chem. 45 (2006) 2055–2060.
[33] S.T. Zheng, D.Q. Yuan, J. Zhang, H.P. Jia, G.Y. Yang, Chem. Commun. (2007) 1858–1860.
[34] J.W. Zhao, H.P. Jia, J. Zhang, S.T. Zheng, G.Y. Yang, Chem. Eur. J. 13 (2007) 10030–10045.
[35] J.W. Zhao, B. Li, S.T. Zheng, G.Y. Yang, Cryst. Growth Des. 7 (2007) 2658–2664.
[36] S.T. Zheng, M.H. Wang, G.Y. Yang, Chem. Asian J. 2 (2007) 1380–1387.
[37] J.W. Zhao, S.T. Zheng, G.Y. Yang, J. Solid State Chem. 180 (2007) 3317–3324.
[38] S.T. Zheng, D.Q. Yuan, J. Zhang, G.Y. Yang, Inorg. Chem. 46 (2007) 4569–4574.
[39] J.W. Zhao, J. Zhang, S.T. Zheng, G.Y. Yang, Chem. Commun. (2008), published online, doi:10.1039/b713510f.
[40] R. Contant, Inorg. Synth. 27 (1990) 108–109.
[41] G.M. Sheldrick, SHELXL-97, Program for Crystal Structure Refinement, University of Göttingen, Göttingen, Germany, 1997.
[42] S. Reinoso, P. Vitoria, L.S. Felices, L. Lezama, J.M. Gutiérrez-Zorrilla, Chem. Eur. J. 11 (2005) 1538–1548.
[43] O.A. Kholdeeva, G.M. Maksimov, R.I. Maksimovskaya, L.A. Kovaleva, M.A. Fedotov, V.A. Grigoriev, C.L. Hill, Inorg. Chem. 39 (2000) 3828–3837.
[44] J.R. Galán-Mascarós, C. Giménez-Saiz, S. Triki, C.J. Gómez-Garcia, E. Coronado, L. Ouahab, Angew. Chem. Int. Ed. Engl. 34 (1995) 1460–1462.
[45] L.S. Felices, P. Vitoria, J.M. Gutiérrez-Zorrilla, L. Lezama, S. Reinoso, Inorg. Chem. 45 (2006) 7748–7757.
[46] L. Lisnard, A. Dolbecq, P. Mialane, J. Marrot, E. Codjovi, F. Sécheresse, Dalton Trans. (2005) 3913–3920.
[47] C. Ritchie, E. Burkholder, P. Kögerler, L. Cronin, Dalton Trans. (2006) 1712–1714.
[48] L. Cronin, Sect. A: Inorg. Chem. 100 (2004) 323–384.
[49] M. Zimmermann, N. Belai, R.J. Butcher, M.T. Pope, E.V. Chubarova, M.H. Dickman, U. Kortz, Inorg. Chem. 46 (2007) 1737–1740.
[50] E. Wang, C. Hu, L. Xu, Introduction of Polyacid Chemistry, Chemical Industry Press, Beijing, 1998.
[51] K. Wassermann, H.J. Lunk, R. Palm, J. Fuchs, N. Steinfeld, R. Stösser, M.T. Pope, Inorg. Chem. 35 (1996) 3273–3279.
[52] N. Belai, M.H. Dickman, M.T. Pope, R. Contant, B. Keita, I.M. Mbomekalle, L. Nadjo, Inorg. Chem. 44 (2005) 169–171.
[53] T. Weakley, Polyhedron 6 (1987) 931–937.
[54] L. Lisnard, A. Dolbecq, P. Mialane, J. Marrot, F. Sécheresse, Inorg. Chim. Acta. 357 (2004) 845–852.
[55] D.E. Billing, B.J. Hathaway, P.J. Nivholls, J. Chem. Soc. A. (1970) 1877–1881.
[56] H. Jin, Y. Qi, E. Wang, Y. Li, C. Qin, X. Wang, S. Chang, Eur. J. Inorg. Chem. (2006) 4541–4545.
[57] E. Burkholder, J. Zubieta, Chem. Commun. (2001) 2056–2057.
[58] H. Jin, Y. Qi, E. Wang, Y. Li, X. Wang, C. Qin, S. Chang, Cryst. Growth Des. 6 (2006) 2693–2698.
[59] H. An, E. Wang, D. Xiao, Y. Li, Z. Su, L. Xu, Angew. Chem. Int. Ed. 45 (2006) 904–908.
[60] S. Reinoso, P. Vitoria, J.M. Gutiérrez-Zorrilla, L. Lezama, L.S. Felices, J.I. Beitia, Inorg. Chem. 44 (2005) 9731–9742.
[61] I. García-Orozco, A.R. Tapia-Benavides, C. Alvarez-Toledano, R.A. Toscano, D. Ramírez-Rosales, R. Zamorano-Ulloa, Y. Reyes-Ortega, J. Mol. Struct. 604 (2002) 57–64.